
Article

Holographic p-Wave Superconductor with Excited States in 4D Einstein–Gauss–Bonnet Gravity

Dong Wang, Xinyi Du, Qiyuan Pan and Jiliang Jing

Special Issue

Black Holes in Einstein–Gauss–Bonnet Theories

Edited by

Prof. Dr. Roman Konoplya



Article

Holographic p-Wave Superconductor with Excited States in 4D Einstein–Gauss–Bonnet Gravity

Dong Wang ^{1,2}, Xinyi Du ^{1,2}, Qiyuan Pan ^{1,2,*}  and Jiliang Jing ^{1,2}

¹ Key Laboratory of Low Dimensional Quantum Structures and Quantum Control of Ministry of Education, Synergetic Innovation Center for Quantum Effects and Applications, Department of Physics, Hunan Normal University, Changsha 410081, China

² Institute of Interdisciplinary Studies, Hunan Normal University, Changsha 410081, China

* Correspondence: panqiyuan@hunnu.edu.cn

Abstract: We construct a holographic p-wave superconductor with excited states in the 4D Einstein–Gauss–Bonnet gravity using the Maxwell complex vector field model. In the probe limit, we observe that, the higher curvature correction or the higher excited state can hinder the vector condensate to be formed in the full parameter space, which is different from the holographic s-wave superconductor. Regardless of the choice of the vector mass by selecting the value of $m^2 L^2$ or $m^2 L_{\text{eff}}^2$, we note that the critical chemical potential becomes evenly spaced for the number of nodes and that the difference of the critical chemical potential between the consecutive states depends on the curvature correction. Moreover, we find that the higher curvature correction or the higher excited state will alter the universal relation of the gap frequency, and the pole and delta function of the conductivity for the excited states can be broadened into the peaks with the finite width as the curvature correction increases.

Keywords: AdS/CFT correspondence; holographic p-wave superconductor; 4D Einstein–Gauss–Bonnet Gravity; excited states

PACS: 11.25.Tq; 04.70.Bw; 74.20.-z



Citation: Wang, D.; Du, X.; Pan, Q.; Jing, J. Holographic p-Wave Superconductor with Excited States in 4D Einstein–Gauss–Bonnet Gravity. *Universe* **2023**, *9*, 104. <https://doi.org/10.3390/universe9020104>

Academic Editor: Roman Konoplya

Received: 19 January 2023

Revised: 12 February 2023

Accepted: 15 February 2023

Published: 17 February 2023



Copyright: © 2023 by the authors. Licensee MDPI, Basel, Switzerland. This article is an open access article distributed under the terms and conditions of the Creative Commons Attribution (CC BY) license (<https://creativecommons.org/licenses/by/4.0/>).

1. Introduction

The holographic correspondence, which is expected to be a version of the anti-de Sitter/conformal field theory (AdS/CFT) correspondence if the bulk is an AdS space [1], shows that the perturbation theory in the bulk and in a theory with one extra dimension can be used to investigate the field theory living on the boundary of AdS with strong coupling [2–4]. In recent years, this correspondence has been extended to explore the phenomena of high-temperature superconductivity [5–8], which is one of the unsolved mysteries in modern condensed matter physics. Neglecting the backreaction of matter fields on the spacetime metric, Hartnoll et al. first built the holographic s-wave superconductor [9] by spontaneously breaking an Abelian gauge symmetry of a charged scalar field in the Schwarzschild-AdS spacetime [10] and successfully reproduced the important properties of a (2 + 1)-dimensional superconductor. Gubser et al. constructed a holographic p-wave superconductor model by introducing an $SU(2)$ Yang–Mills field into the bulk [11], and the authors of [12,13] presented a holographic realization of d-wave superconductivity by introducing a charged massive spin two field propagating in the bulk. Considering a charged vector field into an Einstein–Maxwell theory, Cai et al. introduced a new holographic p-wave superconductor [14] and pointed out that this model is a generalization of the $SU(2)$ model with a general mass and gyromagnetic ratio [15].

It should be noted that the aforementioned holographic superconductor models focus on the ground state that corresponds to the minimum free energy state. More recently, Wang et al. constructed the holographic s-wave superconductor with the excited states in

the probe limit [16] and beyond the probe limit [17], which shows that, as in the evidence of the existence of excited states, the conductivity of each excited state has an additional pole in the imaginary part and a delta function in the real part arising at the low temperature inside the gap. To go a step further, Li et al. studied the non-equilibrium process of the excited states for the holographic s-wave superconductor in detail [18], and we developed a general analytic technique to investigate the excited states of the holographic s-wave and p-wave superconductors [19]. Owing to the importance of the excited states in condensed matter physics, there has been an increasing interest in the excited states regarding the studies of holographic superconductors in the AdS black hole spacetime [20–23] and soliton spacetime [24].

In this work, in order to systematically understand the influences of the $1/N$ or $1/\lambda$ (λ is the 't Hooft coupling) corrections on the holographic dual models, we will generalize the investigation on the excited states in the holographic p-wave superconductor to the $(2+1)$ -dimensional Gauss–Bonnet model inspired by the work of Glavan and Lin [25], where a 4D Einstein–Gauss–Bonnet gravity was introduced by adopting the Gauss–Bonnet coupling parameter α to scale as $1/(D-4)$ in the limit $D \rightarrow 4$. This novel 4D gravity preserves the number of graviton degrees of freedom, thus being free from Ostrogradsky instability, and the Gauss–Bonnet coupling will produce the nontrivial dynamics. However, some independent groups pointed out quite serious doubts regarding the credibility of this 4D Gauss–Bonnet bulk construction since the original claim of [25] explicitly contradicts with the established theorem, i.e., the Lovelock theorem [26–32]. Thus, the researchers further proposed the regularized 4D Einstein–Gauss–Bonnet gravity [33,34] and the consistent $D \rightarrow 4$ Einstein–Gauss–Bonnet gravity [35]. In particular, the consistent theory of $D \rightarrow 4$ Einstein–Gauss–Bonnet gravity, which is also called the 4D Aoki–Gorji–Mukohyama theory of gravity, can be served as a consistent realization of $D \rightarrow 4$ Einstein–Gauss–Bonnet gravity with the rescaled Gauss–Bonnet coupling constant by taking into account all of the above issues [36,37], and recover the black hole solutions provided in [25] and the well-known Friedmann–Lemaître–Robertson–Walker (FLRW) metric. These 4D Einstein–Gauss–Bonnet gravity theories exhibit a number of interesting phenomena in different areas, for reviews, see [38] and the references therein. Interestingly, an exact solution of the same form, named the 4D planar Gauss–Bonnet-AdS black hole, can be obtained via these gravity theories [33–37,39–41]:

$$ds^2 = -f(r)dt^2 + \frac{dr^2}{f(r)} + r^2(dx^2 + dy^2), \quad (1)$$

with the metric coefficient

$$f = f(r) = \frac{r^2}{2\alpha} \left[1 - \sqrt{1 - \frac{4\alpha}{L^2} \left(1 - \frac{r_+^3}{r^3} \right)} \right], \quad (2)$$

where α is the Gauss–Bonnet coupling and r_+ is the black hole horizon related to the Hawking temperature $T_H = 3r_+/(4\pi L^2)$. Since $f \approx r^2(1 - \sqrt{1 - 4\alpha/L^2})/(2\alpha)$, we can define the so-called effective asymptotic AdS scale by [42]

$$L_{\text{eff}}^2 = \frac{2\alpha}{1 - \sqrt{1 - \frac{4\alpha}{L^2}}}, \quad (3)$$

where the upper bound $\alpha = L^2/4$ is the Chern–Simons limit [43]. It should be noted that, since we are interested in the application of the Mermin–Wagner theorem to the holographic superconductors, we prefer the Einstein–Gauss–Bonnet gravity theory, where specific combinations of the curvature tensors are used, over other modified theories, such as the $f(R)$ gravity, where powers of the Ricci scalar only are used [44–46].

As a matter of fact, for the s-wave superconductor, we have constructed the holographic dual model with the excited states away from the probe limit in the 4D Aoki–Gorji–Mukohyama theory of gravity, and observed that the combination of the Gauss–Bonnet gravity and excited state provides richer physics in the scalar condensates and conductivity in the $(2 + 1)$ -dimensional superconductor [47], which exhibits a very interesting and different feature when compared to the higher-dimensional Gauss–Bonnet superconductor [44–46]. Bao et al. studied the excited states of the holographic s-wave superconductor with the scalar field coupled to the Gauss–Bonnet invariance and found that the Gauss–Bonnet coupling has interesting prints on the critical temperature, condensation strength, and optical conductivity for the ground state and excited states [48]. However, the study on the $(2 + 1)$ -dimensional Gauss–Bonnet p-wave superconductor is called for. Thus, we will build the holographic p-wave superconductor in the 4D Einstein–Gauss–Bonnet gravity via the Maxwell complex vector field model and investigate the effects of the curvature corrections on the excited states of the $(2 + 1)$ -dimensional p-wave superconductor. Since the probe limit can extract the main physics of the holographic dual system and avoid the complex computation, we will concentrate on this limit in the following.

This work is organized as follows. In Section 2, we will construct the holographic p-wave superconductor model in the 4D Gauss–Bonnet–AdS black hole background. In Section 3, we will investigate the condensate of the vector field and the phase transition in the $(2 + 1)$ -dimensional Gauss–Bonnet p-wave superconductor both for the ground state and excited states. In Section 4, we will calculate the electrical conductivity of our holographic p-wave model with the excited states. We will conclude, in the last section, with our main results.

2. Description of the p-Wave Model

We will build the holographic p-wave superconductor by using the Maxwell complex vector field model [14,15]:

$$S = \int d^4x \sqrt{-g} \left(-\frac{1}{4} F_{\mu\nu} F^{\mu\nu} - \frac{1}{2} \rho_{\mu\nu}^\dagger \rho^{\mu\nu} - m^2 \rho_\mu^\dagger \rho^\mu + iq\gamma_0 \rho_\mu \rho_\nu^\dagger F^{\mu\nu} \right), \quad (4)$$

with the Maxwell field strength $F_{\mu\nu} = \nabla_\mu A_\nu - \nabla_\nu A_\mu$ and the tensor $\rho_{\mu\nu} = D_\mu \rho_\nu - D_\nu \rho_\mu$. Here, ρ_μ is the complex vector field with mass m and charge q , $D_\mu = \nabla_\mu - iqA_\mu$ denotes the covariant derivative, and γ_0 represents the interaction between the vector field ρ_μ and the gauge field A_μ .

Since we work in a probe limit where the backreaction of matter fields on the spacetime metric is neglected, the gravitational background will be fixed and the matter fields can be treated as the perturbations. Varying the action (4) with respect to the vector field ρ_μ and gauge field A_μ , we have

$$D^\nu \rho_{\nu\mu} - m^2 \rho_\mu + iq\gamma_0 \rho^\nu F_{\nu\mu} = 0, \quad (5)$$

$$\nabla^\nu F_{\nu\mu} - iq(\rho^\nu \rho_{\nu\mu}^\dagger - \rho^{\nu\dagger} \rho_{\nu\mu}) - iq\gamma_0 \nabla^\nu (\rho_\nu \rho_\mu^\dagger - \rho_\nu^\dagger \rho_\mu) = 0. \quad (6)$$

As in [14,15], we also adopt the ansatz for the matter fields $\rho_\mu dx^\mu = \rho_x(r)dx$ and $A_\mu dx^\mu = A_t(r)dt$. Thus, under the metric (1), the above equations of motion become

$$\rho_x'' + \frac{f'}{f} \rho_x' - \frac{1}{f} \left(m^2 - \frac{q^2 A_t^2}{f} \right) \rho_x = 0, \quad (7)$$

$$A_t'' + \frac{2}{r} A_t' - \frac{2q^2 \rho_x^2}{r^2 f} A_t = 0, \quad (8)$$

where the prime denotes the differentiation in r .

In order to investigate the excited states of the holographic p-wave superconductor in the 4D Einstein–Gauss–Bonnet gravity, we have to numerically solve Equations (7) and (8) by using the shooting method [9]. For the boundary condition at the horizon $r = r_+$, the field ρ_x is regular but A_t obeys $A_t(r_+) = 0$. Near the AdS boundary $r \rightarrow \infty$, we obtain the asymptotic behaviors

$$\rho_x = \frac{\rho_{x-}}{r^{\Delta_-}} + \frac{\rho_{x+}}{r^{\Delta_+}}, \quad A_t = \mu - \frac{\rho}{r}, \quad (9)$$

with the characteristic exponents defined by $\Delta_{\pm} = (1 \pm \sqrt{1 + 4m^2L_{\text{eff}}^2})/2$. From the AdS/CFT correspondence, μ and ρ are interpreted as the chemical potential and charge density, and ρ_{x-} and ρ_{x+} correspond to the source and vacuum expectation value of the vector operator O_x in the dual field theory, respectively. In this work, we will impose the boundary condition $\rho_{x-} = 0$ and set $\Delta = \Delta_+$ for clarity.

3. Condensate and Phase Transition

It is well known that a phase transition is a change in state from one phase to another; it can be driven by many parameters, such as the temperature, pressure, etc. Choosing the temperature as the driving parameter, one finds that the high-temperature phase is almost always more disordered, i.e., has a higher symmetry than the low-temperature phase. In the holographic superconductor model, a charged condensate forms below a critical temperature T_c , which is the symmetry breaking phase transition to a superconducting phase. Now, we are in a position to generalize the investigation on the vector condensate and phase transition for the ground state of the holographic p-wave superconductor in the 4D Einstein–Gauss–Bonnet gravity [49] to those for the excited states. When performing numerical calculations, we will use the following scaling symmetries

$$\begin{aligned} r &\rightarrow \lambda r, \quad (t, x, y) \rightarrow \lambda^{-1}(t, x, y), \quad q \rightarrow q, \quad (\rho_x, A_t) \rightarrow \lambda(\rho_x, A_t), \\ \mu &\rightarrow \lambda\mu, \quad \rho \rightarrow \lambda^2\rho, \quad \rho_{x+} \rightarrow \lambda^{1+\Delta}\rho_{x+}, \end{aligned} \quad (10)$$

to build the invariant and dimensionless quantities, where λ is a real positive number. For simplicity, we set $r_+ = 1$ and $q = 1$ in the following calculation. On the other hand, from [49], we observe that, regardless of the choice of the mass of the vector field, by choosing the value of m^2L^2 or $m^2L_{\text{eff}}^2$, the critical temperature T_c decreases as α increases for all vector field masses in the ground state. We will check it in the excited states and expect this tendency to be the same. For concreteness, we choose the Gauss–Bonnet parameter in the range $-L^2/10 \leq \alpha \leq L^2/4$ as in [49] and fix the masses of the vector field $m^2L^2 = 3/4$ and $m^2L_{\text{eff}}^2 = 3/4$ in our calculation. It should be noted that the other choices of the vector mass will not qualitatively modify our results.

In Figure 1, we present the condensates of the vector operator O_x as a function of temperature for various Gauss–Bonnet parameters α from the ground state ($n = 0$) to the second excited state ($n = 2$) with the fixed vector masses $m^2L^2 = 3/4$ and $m^2L_{\text{eff}}^2 = 3/4$. Obviously, there exists the critical behavior of the second-order phase transition $\langle O_x \rangle \sim (1 - T/T_c)^{1/2}$ for the fixed α and n , and each curve is in agreement with that of the holographic p-wave superconducting phase in the literature, where the condensate goes to a constant at zero temperature. For the fixed number of nodes n , we observe that this constant, which corresponds to the condensation gap, increases as α increases, which suggests that, regardless of the ground state or the excited states, the higher curvature correction causes the vector hair to be more difficult to be developed in the $(2+1)$ -dimensional p-wave superconductor. This result is independent of the choice of the vector mass by selecting the value of m^2L^2 or $m^2L_{\text{eff}}^2$, which can be used to back up the numerical finding as shown in [49] for the ground state of the $(2+1)$ -dimensional Gauss–Bonnet superconductor. For the fixed Gauss–Bonnet parameter α , we see that the condensation gap increases as n increases, which indicates that the higher excited state causes it to be harder for the condensate of the vector operator to form. Thus, the p-wave superconductor still exists

even when we consider the Gauss–Bonnet corrections to the standard $(2 + 1)$ -dimensional holographic superconductor model with the excited states.

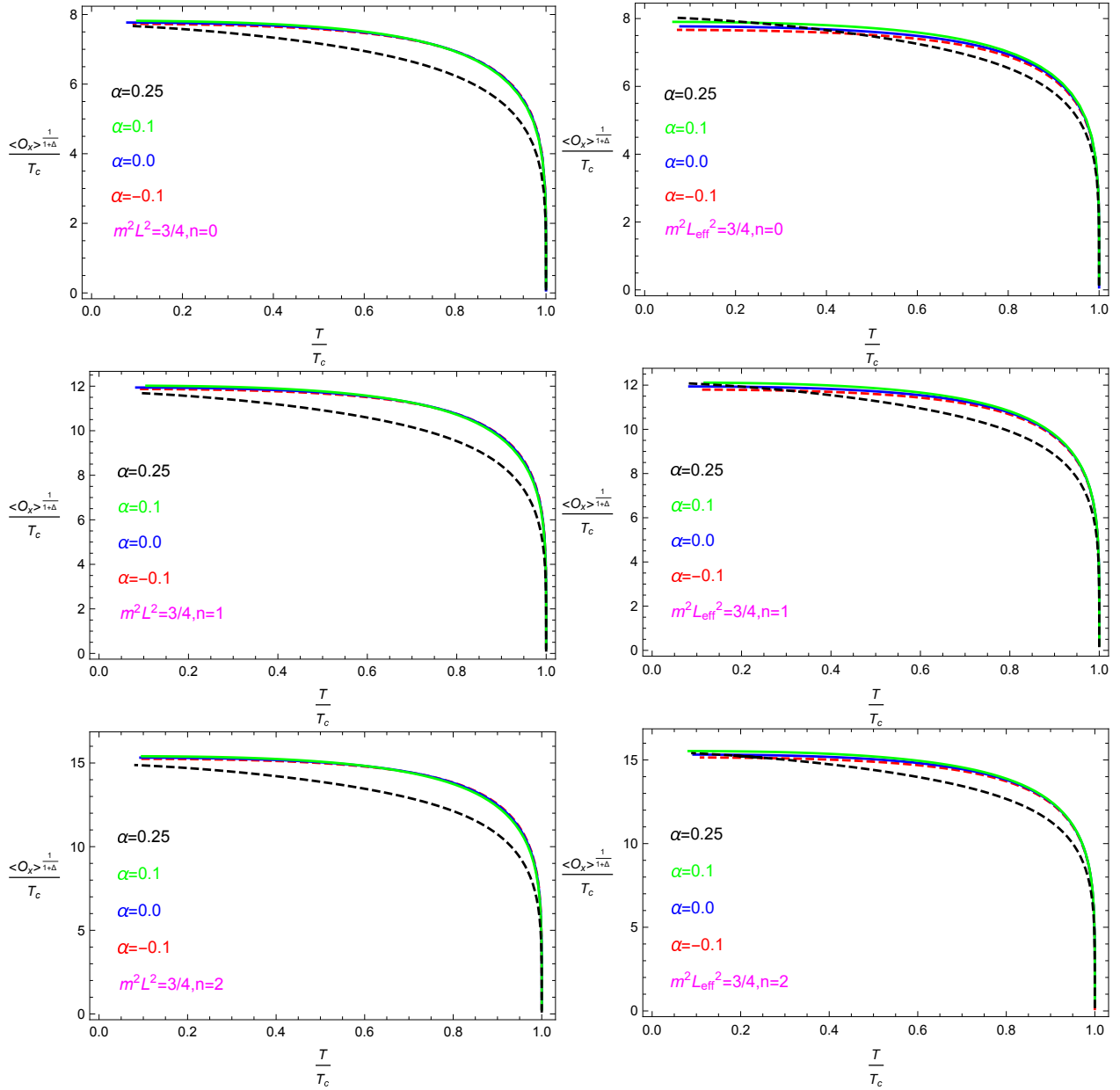


Figure 1. (Color online) The condensates of the vector operator O_x as a function of temperature for the masses of the vector field $m^2 L^2 = 3/4$ (**left**) and $m^2 L_{\text{eff}}^2 = 3/4$ (**right**) with different values of the Gauss–Bonnet parameter from the ground state to the second excited state. In each panel, the four lines correspond to increasing Gauss–Bonnet parameters, i.e., $\alpha = -0.1$ (red and dashed), 0.0 (blue), 0.1 (green), and 0.25 (black and dashed), respectively.

In order to further support the observation obtained in Figure 1, we provide the critical temperature T_c as a function of the Gauss–Bonnet parameter from the ground state ($n = 0$) to the third excited state ($n = 3$) for the fixed vector masses $m^2 L^2 = 3/4$ and $m^2 L_{\text{eff}}^2 = 3/4$ in Figure 2. It is shown that, regardless of the choice of the mass of the vector field by choosing the value of $m^2 L^2$ or $m^2 L_{\text{eff}}^2$, we find that the increase in the Gauss–Bonnet parameter α or the number of nodes n results in the decrease in the critical temperature T_c , which can be used to back up the numerical finding as shown in Figure 1 that the higher curvature correction or the higher excited state can hinder the condensate to be formed

in the full parameter space. This behavior is reminiscent of that seen for the s-wave case where the curvature correction has a more subtle effect, i.e., the critical temperature first decreases then increases as the curvature correction tends toward the Chern–Simons value. Increasing n will weaken this subtle effect of the Gauss–Bonnet parameter on the critical temperature [47], so we conclude that the curvature correction has completely different effects on the critical temperature T_c for the s-wave and p-wave superconductors with the excited states in $(2 + 1)$ -dimensions.

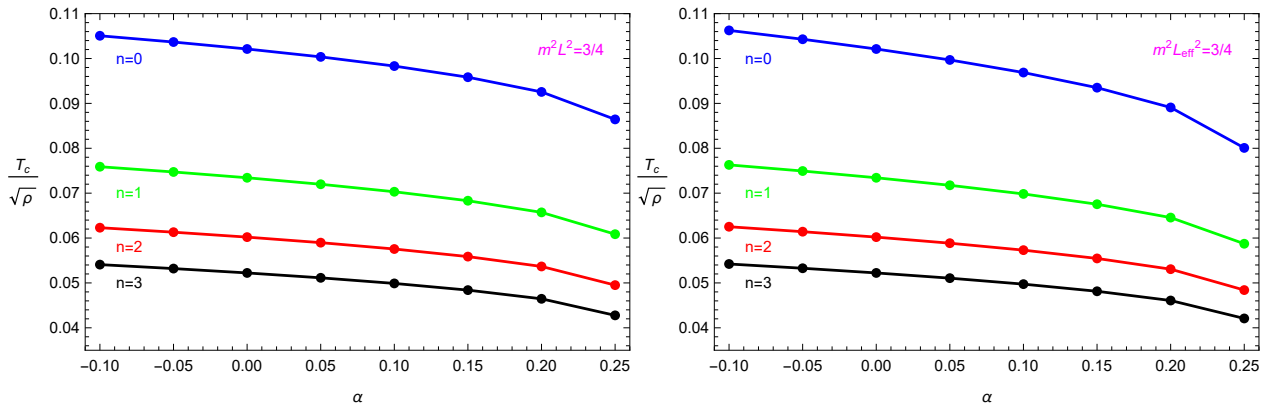


Figure 2. (Color online) The critical temperature T_c of the vector operator O_x as a function of the Gauss–Bonnet parameter for the fixed masses of the vector field $m^2 L^2 = 3/4$ (left) and $m^2 L_{\text{eff}}^2 = 3/4$ (right) from the ground state to the third excited state.

As a matter of fact, we can also realize the phase transition of the holographic superconductor around the critical chemical potential μ_c , above which the vector field begins to condense. Therefore, we present the critical chemical potential μ_c of the vector operator O_x with the masses of the vector field $m^2 L^2 = 3/4$ and $m^2 L_{\text{eff}}^2 = 3/4$ from the ground state to the 20-th excited state for different values of the Gauss–Bonnet parameter, i.e., $\alpha = -0.10, 0, 0.10$, and 0.25 in Table 1. It is found that the critical chemical potential μ_c increases with the increase in α or n , which agrees well with the finding of the critical temperature T_c and indicates that the higher curvature correction or the higher excited state causes the condensate of the vector operator O_x to be harder. Obviously, the critical chemical potential μ_c of $m^2 L^2 = 3/4$ (left column) is much closer to that of $m^2 L_{\text{eff}}^2 = 3/4$ (right column) as the number of nodes n increases for each α , for example, in the case of $n = 20$ here, which means that, regardless of the choice of the mass by selecting the value of $m^2 L^2$ or $m^2 L_{\text{eff}}^2$, the critical chemical potentials are the same for a sufficiently large n . Fitting the relation between μ_c and n by using the results in Table 1, we have

$$\mu_c \approx \begin{cases} 4.820n + 5.042, & \text{for } \alpha = -0.10, \\ 5.189n + 5.345, & \text{for } \alpha = 0.00, \\ 5.714n + 5.772, & \text{for } \alpha = 0.10, \\ 7.931n + 7.391, & \text{for } \alpha = 0.25, \end{cases} \quad (11)$$

for the vector mass $m^2 L^2 = 3/4$ and

$$\mu_c \approx \begin{cases} 4.821n + 4.941, & \text{for } \alpha = -0.10, \\ 5.189n + 5.345, & \text{for } \alpha = 0.00, \\ 5.712n + 5.927, & \text{for } \alpha = 0.10, \\ 7.919n + 8.479, & \text{for } \alpha = 0.25, \end{cases} \quad (12)$$

for the vector mass $m^2 L_{\text{eff}}^2 = 3/4$, which shows that the critical chemical potential μ_c becomes evenly spaced for the number of nodes n and that the difference of μ_c between the consecutive states does not depend on the choice of the vector mass but does depend on the Gauss–Bonnet parameter, i.e., $\Delta\mu_c = 4.8$ for $\alpha = -0.10$, $\Delta\mu_c = 5.2$ for $\alpha = 0.00$, $\Delta\mu_c = 5.7$ for $\alpha = 0.10$, and $\Delta\mu_c = 7.9$ for $\alpha = 0.25$. Interestingly, increasing the Gauss–Bonnet parameter α increases this difference of the critical chemical potential between the consecutive states.

Table 1. The critical chemical potential μ_c of the vector operator O_x for the masses of the vector field $m^2 L^2 = 3/4$ (left column) and $m^2 L_{\text{eff}}^2 = 3/4$ (right column) with different values of the Gauss–Bonnet parameter from the ground state to the 20-th excited state. It should be noted that the critical chemical potentials for the different choices of the vector mass are the same for the case of $\alpha = 0$, i.e., the Schwarzschild-AdS black hole.

n	$\alpha = -0.10$	$\alpha = 0$	$\alpha = 0.10$	$\alpha = 0.25$
0	5.163	5.047	5.465	5.896
1	9.896	9.790	10.569	11.527
2	14.682	14.581	15.723	17.203
3	19.486	19.389	20.894	22.897
4	24.298	24.203	26.074	28.601
5	29.115	29.021	31.258	34.309
6	33.934	33.842	36.445	40.021
7	38.755	38.664	41.635	45.735
8	43.578	43.488	46.825	51.451
9	48.401	48.312	52.016	57.168
10	53.225	53.136	57.208	62.886
11	58.050	57.961	62.401	68.604
12	62.875	62.787	67.594	74.323
13	67.700	67.612	72.788	80.042
14	72.526	72.438	77.982	85.762
15	77.351	77.264	83.176	91.482
16	82.177	82.090	88.370	97.203
17	87.003	86.916	93.565	102.923
18	91.829	91.743	98.759	108.644
19	96.656	96.569	103.954	114.365
20	101.482	101.396	109.149	120.086

4. Conductivity

In order to calculate the conductivity of the $(2 + 1)$ -dimensional Gauss–Bonnet p-wave superconductor with the excited states, we assume that the perturbed Maxwell field has a form $\delta A_y = e^{-i\omega t} A_y(r) dy$, just as in [14]. Thus, the equation of motion of the perturbation $A_y(r)$ is

$$A_y'' + \frac{f'}{f} A_y' + \left(\frac{\omega^2}{f^2} - \frac{2q^2 \rho_x^2}{r^2 f} \right) A_y = 0. \quad (13)$$

At the horizon, we impose the ingoing wave boundary condition $A_y(r) \sim f(r)^{-i\omega/(4\pi T_H)}$. At the asymptotic boundary ($r \rightarrow \infty$), we obtain

$$A_y = A^{(0)} + \frac{A^{(1)}}{r}, \quad (14)$$

which leads to the conductivity of the dual superconductor

$$\sigma = -\frac{iA^{(1)}}{\omega A^{(0)}}. \quad (15)$$

Considering that the different choices of the vector mass do not qualitatively modify the effect of the Gauss–Bonnet correction on the behavior of the condensates for the vector operator O_x , we will fix the mass of the vector field by $m^2 L_{\text{eff}}^2 = 3/4$ in this section.

In Figure 3, we plot the conductivity of the $(2+1)$ -dimensional p-wave superconductor for the vector mass $m^2 L_{\text{eff}}^2 = 3/4$ with different values of the Gauss–Bonnet parameter from the ground state to the third excited state at temperature $T/T_c \approx 0.20$. It is shown that, similar to the ground state [49], there also exists a gap in the conductivity of the excited state and the gap frequency ω_g increases as the Gauss–Bonnet parameter α increases, where we define the gap frequency ω_g as the frequency minimizing $\text{Im}[\sigma(\omega)]$ [50]. Obviously, the increasing Gauss–Bonnet parameter α or number of nodes n is to increase ω_g/T_c , which implies that the higher curvature correction or the higher excited state will alter the universal relation $\omega_g/T_c \approx 8$ [50] for the $(2+1)$ -dimensional p-wave superconductor. Moreover, we find that, as evidence of the existence of excited states, there exist additional poles in $\text{Im}[\sigma(\omega)]$ and delta functions in $\text{Re}[\sigma(\omega)]$ arising at low temperatures for the excited states, which is similar to the holographic s-wave superconductor with the excited states [16,17]. Interestingly, as α increases, we clearly see that the pole and delta function can be broadened into the peaks with the finite width, which is consistent with the finding in the $(2+1)$ -dimensional Gauss–Bonnet s-wave superconductor with the excited states [47]. This may be a quite general feature for the holographic superconductor with the excited states in the 4D Einstein–Gauss–Bonnet gravity.

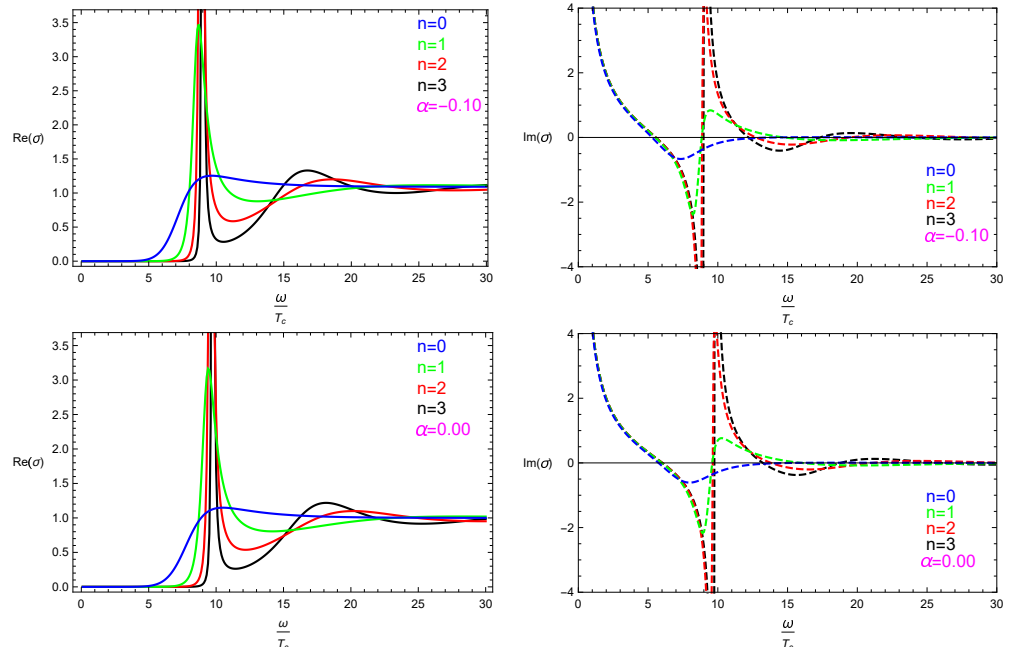


Figure 3. Cont.

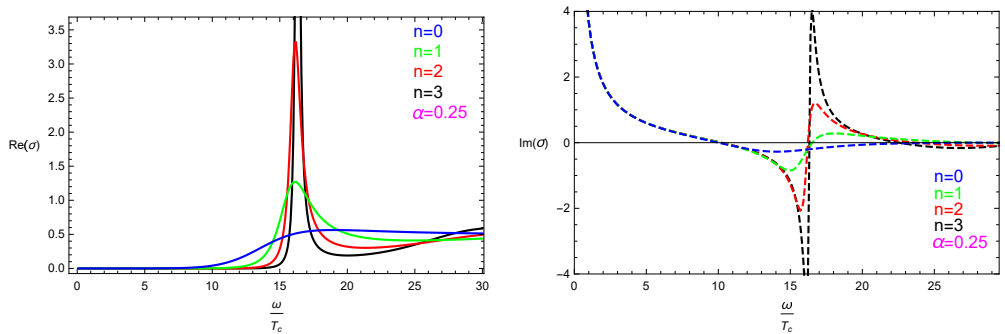


Figure 3. (Color online) The conductivity for the mass of the vector field $m^2 L_{\text{eff}}^2 = 3/4$ with different values of the Gauss–Bonnet parameter from the ground state to the third excited state, where the solid line and dashed line represent the real part and imaginary part of the conductivity $\sigma(\omega)$. In each panel, the blue, green, red, and black lines denote the ground ($n = 0$), first ($n = 1$), second ($n = 2$), and third ($n = 3$) states, respectively.

5. Conclusions

In order to understand the influences of the $1/N$ or $1/\lambda$ corrections on the vector condensate, we have built the $(2 + 1)$ -dimensional p-wave superconductor with the excited states in the 4D Einstein–Gauss–Bonnet gravity using the Maxwell complex vector field model. In the probe limit, regardless of the choice of the mass of the vector field by choosing the value of $m^2 L^2$ or $m^2 L_{\text{eff}}^2$, the system undergoes a second-order phase transition near the critical temperature T_c both for the ground state and excited states. We noted that, different from the holographic s-wave superconductor where the Gauss–Bonnet parameter α and the number of nodes n have a more subtle effect on the critical temperature, in the holographic p-wave case, the critical temperature T_c always decreases as α or n increases in the full parameter space. This means that the curvature corrections have completely different effects on the critical temperature T_c for the s-wave and p-wave superconductors with the excited states in $(2 + 1)$ -dimensions and implies that the higher curvature correction or the higher excited state will cause the vector hair to be more difficult to develop. We also calculated the critical chemical potential μ_c of the excited states, and found that μ_c becomes evenly spaced for the number of nodes n and that the difference of μ_c between the consecutive states is independent of the choice of the vector mass but dependent of the Gauss–Bonnet parameter α , i.e., increasing α increases the difference of μ_c between the consecutive states. Furthermore, we investigated the conductivity of the system and showed that the gap frequency ω_g/T_c increases with the increase in the Gauss–Bonnet parameter α or number of nodes n , which indicates that the higher curvature correction or the higher excited state will alter the universal relation $\omega_g/T_c \approx 8$ for the $(2 + 1)$ -dimensional p-wave superconductors. Interestingly, we observed that, as the Gauss–Bonnet parameter α increases, the pole in the imaginary part of the conductivity and delta function in the real part for the excited states can be broadened into the peaks with the finite width, which agrees well with the finding in the $(2 + 1)$ -dimensional Gauss–Bonnet s-wave superconductor with the excited states. This may be a quite general feature for the holographic superconductors with the excited states in the 4D Einstein–Gauss–Bonnet gravity.

Author Contributions: Investigation, D.W., X.D., Q.P. and J.J.; writing—original draft preparation, D.W. and X.D.; writing—review and editing, Q.P.; supervision, Q.P. and J.J. All authors have read and agreed to the published version of the manuscript.

Funding: This work was supported by the National Key Research and Development Program of China (Grant No. 2020YFC2201400), National Natural Science Foundation of China (Grant Nos. 12275079, 12035005 and 11690034) and Postgraduate Scientific Research Innovation Project of Hunan Province (Grant No. CX20210472).

Data Availability Statement: Not applicable.

Conflicts of Interest: The authors declare no conflict of interest.

References

1. Bousso, R. The holographic principle. *Rev. Mod. Phys.* **2002**, *74*, 825. [\[CrossRef\]](#)
2. Maldacena, J. The large-N limit of superconformal field theories and supergravity. *Int. J. Theor. Phys.* **1999**, *38*, 1113. [\[CrossRef\]](#)
3. Witten, E. Anti-de Sitter space and holography. *Adv. Theor. Math. Phys.* **1998**, *2*, 253. [\[CrossRef\]](#)
4. Gubser, S.S.; Klebanov, I.R.; Polyakov, A.M. Gauge theory correlators from non-critical string theory. *Phys. Lett. B* **1998**, *428*, 105. [\[CrossRef\]](#)
5. Hartnoll, S.A. Lectures on holographic methods for condensed matter physics. *Class. Quant. Grav.* **2009**, *26*, 224002. [\[CrossRef\]](#)
6. Herzog, C.P. Lectures on Holographic Superfluidity and Superconductivity. *J. Phys. A* **2009**, *42*, 343001. [\[CrossRef\]](#)
7. Horowitz, G.T. Introduction to Holographic Superconductors. *Lect. Notes Phys.* **2011**, *828*, 313.
8. Cai, R.G.; Li, L.; Li, L.F.; Yang, R.Q. Introduction to Holographic Superconductor Models. *Sci. China Phys. Mech. Astron.* **2015**, *58*, 060401. [\[CrossRef\]](#)
9. Hartnoll, S.A.; Herzog, C.P.; Horowitz, G.T. Building a Holographic Superconductor. *Phys. Rev. Lett.* **2008**, *101*, 031601. [\[CrossRef\]](#)
10. Gubser, S.S. Breaking an Abelian gauge symmetry near a black hole horizon. *Phys. Rev. D* **2008**, *78*, 065034. [\[CrossRef\]](#)
11. Gubser, S.S.; Pufu, S.S. The gravity dual of a p-wave superconductor. *J. High Energy Phys.* **2008**, *11*, 33. [\[CrossRef\]](#)
12. Chen, J.W.; Kao, Y.J.; Maity, D.; Wen, W.Y.; Yeh, C.P. Towards a holographic model of d-wave superconductors. *Phys. Rev. D* **2010**, *81*, 106008. [\[CrossRef\]](#)
13. Benini, F.; Herzog, C.P.; Rahman, R.; Yarom, A. Gauge gravity duality for d-wave superconductors: Prospects and challenges. *J. High Energy Phys.* **2010**, *11*, 137. [\[CrossRef\]](#)
14. Cai, R.G.; He, S.; Li, L.; Li, L.F. A holographic study on vector condensate induced by a magnetic field. *J. High Energy Phys.* **2013**, *12*, 36. [\[CrossRef\]](#)
15. Cai, R.G.; Li, L.; Li, L.F. A holographic p-wave superconductor model. *J. High Energy Phys.* **2014**, *1*, 32. [\[CrossRef\]](#)
16. Wang, Y.Q.; Hu, T.T.; Liu, Y.X.; Yang, J.; Zhao, L. Excited states of holographic superconductors. *J. High Energy Phys.* **2020**, *6*, 13. [\[CrossRef\]](#)
17. Wang, Y.Q.; Li, H.B.; Liu, Y.X.; Zhong, Y. Excited states of holographic superconductors with backreaction. *Eur. Phys. J. C* **2021**, *81*, 628. [\[CrossRef\]](#)
18. Li, R.; Wang, J.; Wang, Y.Q.; Zhang, H.B. Nonequilibrium dynamical transition process between excited states of holographic superconductors. *J. High Energy Phys.* **2020**, *11*, 59. [\[CrossRef\]](#)
19. Qiao, X.Y.; Wang, D.; OuYang, L.; Wang, M.J.; Pan, Q.Y.; Jing, J.L. An analytic study on the excited states of holographic superconductors. *Phys. Lett. B* **2020**, *811*, 135864. [\[CrossRef\]](#)
20. Xiang, Q.; Zhao, L.; Wang, Y.Q. Excited states of holographic superconductors from massive gravity. *Commun. Theor. Phys.* **2022**, *74*, 115401. [\[CrossRef\]](#)
21. Zhang, S.H.; Zhao, Z.X.; Pan, Q.Y.; Jing, J.L. Excited states of holographic superconductors with hyperscaling violation. *Nucl. Phys. B* **2022**, *976*, 115701. [\[CrossRef\]](#)
22. Nguyen, T.T.; Phat, T.H. Asymptotic critical behavior of holographic phase transition at finite topological charge—the spectrum of excited states becomes continuous at $T = 0$. *J. High Energy Phys.* **2022**, *6*, 4. [\[CrossRef\]](#)
23. Xiang, Q.; Zhao, L.; Wang, Y.Q. Spontaneously Translational Symmetry Breaking in the Excited States of Holographic Superconductor. *arXiv* **2022**, arXiv:2207.10593.
24. Ouyang, L.; Wang, D.; Qiao, X.Y.; Wang, M.J.; Pan, Q.Y.; Jing, J.L. Holographic Insulator/Superconductor Phase Transitions with Excited States. *Sci. China Phys. Mech. Astron.* **2021**, *64*, 240411. [\[CrossRef\]](#)
25. Glavan, D.; Lin, C.S. Einstein–Gauss–Bonnet Gravity in Four-Dimensional Spacetime. *Phys. Rev. Lett.* **2020**, *124*, 081301. [\[CrossRef\]](#)
26. Gürses, M.; Şişman, T.Ç.; Tekin, B. Is there a novel Einstein–Gauss–Bonnet theory in four dimensions? *Eur. Phys. J. C* **2020**, *80*, 647. [\[CrossRef\]](#)
27. Ai, W.Y. A note on the novel 4D Einstein–Gauss–Bonnet gravity. *Commun. Theor. Phys.* **2020**, *72*, 095402. [\[CrossRef\]](#)
28. Mahapatra, S. A note on the total action of 4D Gauss–Bonnet theory. *Eur. Phys. J. C* **2020**, *80*, 992. [\[CrossRef\]](#)
29. Shu, F.W. Vacua in novel 4D Einstein–Gauss–Bonnet Gravity: Pathology and instability? *Phys. Lett. B* **2020**, *811*, 135907. [\[CrossRef\]](#)
30. Tian, S.X.; Zhu, Z.H. Non-full equivalence of the four-dimensional Einstein–Gauss–Bonnet gravity and Horndeksi gravity for Bianchi type I metric. *arXiv* **2020**, arXiv:2004.09954.
31. Arrechea, J.; Delhom, A.; Jiménez-Cano, A. Inconsistencies in four-dimensional Einstein–Gauss–Bonnet gravity. *Chin. Phys. C* **2021**, *45*, 013107. [\[CrossRef\]](#)
32. Gürses, M.; Şişman, T.Ç.; Tekin, B. Comment on “Einstein–Gauss–Bonnet Gravity in Four-Dimensional Spacetime”. *Phys. Rev. Lett.* **2020**, *125*, 149001. [\[CrossRef\]](#) [\[PubMed\]](#)
33. Lu, H.; Pang, Y. Horndeski Gravity as $D \rightarrow 4$ Limit of Gauss–Bonnet. *Phys. Lett. B* **2020**, *809*, 135717. [\[CrossRef\]](#)
34. Hennigar, R.A.; Kubiznak, D.; Mann, R.B.; Pollack, C. On Taking the $D \rightarrow 4$ limit of Gauss–Bonnet Gravity: Theory and Solutions. *J. High Energy Phys.* **2020**, *7*, 27. [\[CrossRef\]](#)
35. Aoki, K.; Gorji, M.A.; Mukohyama, S. A consistent theory of $D \rightarrow 4$ Einstein–Gauss–Bonnet gravity. *Phys. Lett. B* **2020**, *810*, 135843. [\[CrossRef\]](#)
36. Aoki, K.; Gorji, M.A.; Mukohyama, S. Cosmology and gravitational waves in consistent $D \rightarrow 4$ Einstein–Gauss–Bonnet gravity. *J. Cosmol. Astropart. Phys.* **2020**, *9*, 14. [\[CrossRef\]](#)

37. Aoki, K.; Gorji, M.A.; Mizuno, S.; Mukohyama, S. Inflationary gravitational waves in consistent $D \rightarrow 4$ Einstein–Gauss–Bonnet gravity. *J. Cosmol. Astropart. Phys.* **2021**, *1*, 54. [[CrossRef](#)]
38. Fernandes, P.G.S.; Carrilho, P.; Clifton, T.; Mulryne, D.J. The 4D Einstein–Gauss–Bonnet theory of gravity: A review. *Class. Quantum Grav.* **2022**, *39*, 063001. [[CrossRef](#)]
39. Konoplya, R.A.; Zhidenko, A. Black holes in the four-dimensional Einstein–Lovelock gravity. *Phys. Rev. D* **2020**, *101*, 084038. [[CrossRef](#)]
40. Fernandes, P.G.S. Charged Black Holes in AdS Spaces in 4D Einstein Gauss–Bonnet Gravity. *Phys. Lett. B* **2020**, *805*, 135468. [[CrossRef](#)]
41. Konoplya, R.A.; Zhidenko, A. 4D Einstein–Lovelock black holes: Hierarchy of orders in curvature. *Phys. Lett. B* **2020**, *807*, 135607. [[CrossRef](#)]
42. Cai, R.G. Gauss–Bonnet black holes in AdS spaces. *Phys. Rev. D* **2002**, *65*, 084014. [[CrossRef](#)]
43. Crisostomo, J.; Troncoso, R.; Zanelli, J. Black hole scan. *Phys. Rev. D* **2000**, *62*, 084013. [[CrossRef](#)]
44. Gregory, R.; Kanno, S.; Soda, J. Holographic superconductors with higher curvature corrections. *J. High Energy Phys.* **2009**, *10*, 10. [[CrossRef](#)]
45. Pan, Q.Y.; Wang, B.; Papantonopoulos, E.; Oliveria, J.; Pavan, A.B. Holographic superconductors with various condensates in Einstein–Gauss–Bonnet gravity. *Phys. Rev. D* **2010**, *81*, 106007. [[CrossRef](#)]
46. Brihaye, Y.; Hartmann, B. Holographic superconductors in 3 + 1 dimensions away from the probe limit. *Phys. Rev. D* **2010**, *81*, 126008. [[CrossRef](#)]
47. Pan, J.; Qiao, X.Y.; Wang, D.; Pan, Q.Y.; Nie, Z.Y.; Jing, J.L. Holographic superconductors in 4D Einstein–Gauss–Bonnet gravity with backreactions. *Phys. Lett. B* **2021**, *823*, 136755. [[CrossRef](#)]
48. Bao, Y.; Guo, H.; Kuang, X.M. Excited states of holographic superconductor with scalar field coupled to Gauss–Bonnet invariance. *Phys. Lett. B* **2021**, *822*, 136646. [[CrossRef](#)]
49. Qiao, X.Y.; OuYang, L.; Wang, D.; Pan, Q.Y.; Jing, J.L. Holographic superconductors in 4D Einstein–Gauss–Bonnet gravity. *J. High Energy Phys.* **2020**, *12*, 192. [[CrossRef](#)]
50. Horowitz, G.T.; Roberts, M.M. Holographic superconductors with various condensates. *Phys. Rev. D* **2008**, *78*, 126008. [[CrossRef](#)]

Disclaimer/Publisher’s Note: The statements, opinions and data contained in all publications are solely those of the individual author(s) and contributor(s) and not of MDPI and/or the editor(s). MDPI and/or the editor(s) disclaim responsibility for any injury to people or property resulting from any ideas, methods, instructions or products referred to in the content.